Anadolu Orman Araştırmaları Dergisi
Anatolian Journal of Forest Research
http://dergipark.org.tr/ajfr

Evaluating the performance of the EUMETSAT H SAF H35 fractional snow-covered area product over the Tibetan Plateau

Semih Kuter[1*], Çağrı Hasan Karaman[2], Mustafa Berkay Akpınar[3], Zuhal Akyürek[3,4]

[1] Çankırı Karatekin University, Faculty of Forestry, Department of Forest Engineering, Çankırı, Türkiye
[2] HidroSAF Ltd., Middle East Technical University Technopolis, Ankara, Türkiye
[3] Middle East Technical University, Faculty of Engineering, Department of Civil Engineering, Ankara, Türkiye
[4] Middle East Technical University, Department of Geodetic and Geographic Information Technologies, Ankara, Türkiye

ARTICLE INFO
Received: 11/10/2024
Accepted: 09/12/2024
https://doi.org/10.53516/ajfr.1565569
*Corresponding author:
semihkuter@karatekin.edu.tr

ABSTRACT **Research Article**

Background and aims This study evaluates the performance of the H35 fractional snow-covered area (fSCA) product over the Tibetan Plateau (TP) from May 2019 to December 2021. The H35 product, derived from AVHRR satellite data, provides daily fSCA estimates at a resolution of 0.01°. The aim of this work is to assess the accuracy and reliability of this product in capturing snow cover dynamics over a significant period.
Methods Validation of the H35 product uses a high-resolution, cloud-free snow cover dataset derived from long-term MODIS data, ensuring temporal consistency and high accuracy. Statistical metrics, including probability of detection (POD), false alarm ratio (FAR), and accuracy (ACC), were employed to assess the product's performance.
Results The results reveal seasonal variations in performance, with POD values reaching a peak of 0.91 during the winter months. The FAR shows an inverse trend, while the overall ACC values remain consistently high, indicating reliable performance across the study period.
Conclusions This study contributes to the understanding of snow cover dynamics over the TP and highlights the significance of validating satellite-derived products for hydrological studies. The consistently high accuracy of the H35 product underscores its potential for use in monitoring snow cover in the region.

Key Words: Optical remote sensing of snow, EUMETSAT, H SAF, fractional snow cover, H35

EUMETSAT H SAF H35 fraksiyonel karla kaplı alan ürününün Tibet Platosu üzerinde performansının değerlendirilmesi

ÖZ

Giriş ve Hedefler Tibet Platosu (TP) üzerindeki kar örtüsü dinamiklerini anlamak, hidrolojik çalışmalar ve iklim modellemeleri için kritik öneme sahiptir. Bu çalışma, H35 fraksiyonel karla kaplı alan (fSCA) ürününün Mayıs 2019 ile Aralık 2021 arasındaki performansını değerlendirmeyi amaçlamaktadır. H35 ürünü, AVHRR uydu verilerinden türetilmiş olup, 0,01° çözünürlükte günlük fSCA tahminleri sunmaktadır.
Yöntemler Değerlendirme, uzun vadeli MODIS verilerinden türetilen yüksek çözünürlüklü ve bulutsuz bir kar örtüsü veri seti kullanılarak gerçekleştirilmiştir. İstatistiksel analizde algılama olasılığı (POD), yanlış alarm oranı (FAR) ve doğruluk (ACC) gibi metrikler kullanılmıştır.
Bulgular Sonuçlar H35 ürününün performansında mevsimsel değişimlere işaret etmektedir. Kış aylarında POD değerleri 0,91'e ulaşırken, FAR düşüş eğilimi göstermiştir. Genel doğruluk (ACC) değerleri ise sürekli olarak yüksek seviyede kalmıştır, bu da ürünün güvenilirliğini ortaya koymaktadır.
Sonuçlar H35 ürününün doğrulama sonuçları, TP üzerindeki kar örtüsü dinamiklerinin anlaşılmasına katkı sağlamaktadır. Ayrıca, uydu verilerinden türetilen ürünlerin doğruluk analizinin, özellikle hidrolojik çalışmalar bağlamında, önemini vurgulamaktadır.

Anahtar Kelimeler: Karın optik uzaktan algılanması, EUMETSAT, H SAF, fraksiyonel kar örtüsü, H35

Citing this article:
Kuter, S., Karaman, Ç.H., Akpınar, M.B., Akyürek, Z., 2024. Evaluating the performance of the EUMETSAT H SAF H35 fractional snow-covered area product over the Tibetan Plateau. Anatolian Journal of Forest Research, 10(2), 148-156.

1. Introduction

Snow cover is a key component of the Earth's cryosphere, influencing global climate and water cycles. Each year, seasonal snow covers a substantial part of the Earth's surface, accounting for about 31% of the total land area and 40% of the terrestrial area in the Northern Hemisphere (Hall *et al.*, 1995; Breen *et al.*, 2023). The spatial extent of snow cover can vary considerably both within and between years (Wang *et al.*, 2018). Recent research efforts indicate a general decline in global snow coverage, primarily attributed to a warming climate (Wang *et al.*, 2018; Pulliainen *et al.*, 2020). However, these changes in snow extent differ significantly across various regions (Brown and Mote, 2009).

Globally, monitoring and mapping of snow cover are crucial for understanding the Earth's energy balance and the role of snow in the climate system. Snow has a high albedo, reflecting a large portion of incoming solar radiation back into the atmosphere (Tekeli *et al.*, 2005; Kuter *et al.*, 2018). This property is essential in regulating the Earth's surface heating and cooling patterns. Among all land surface types, snow cover has the most significant impact on the surface energy balance (Chen *et al.*, 2021). The presence or absence of snow can notably alter this energy balance, leading to changes in climate and related feedback mechanisms. Therefore, changes in snow cover extent and duration significantly affect the Earth's energy balance and global climate (Takala *et al.*, 2011). Accurate snow cover monitoring and mapping are vital for improving our understanding of these processes and their influence on the Earth's climate system.

Two key snow parameters, i.e., snow-covered area (SCA) and snow water equivalent (SWE), can be retrieved globally by space-borne instruments operating at visible and microwave frequencies. SWE, which quantifies the amount of liquid water within the snowpack, is determined using active and passive microwave techniques (Pulliainen and Hallikainen, 2001; Saberi *et al.*, 2020). SCA, representing the spatial distribution of snow, are derived from multispectral optical remote sensing data, and further categorized into two types: *i)* binary snow cover, indicating the presence or absence of snow (i.e., snow/no snow), and *ii*) sub-pixel snow cover, which measures the fractional snow-covered area (fSCA) as the percentage of snow within a pixel's footprint (Metsämäki *et al.*, 2015). The latter estimates the fractional snow-covered area within each pixel by analyzing the spectral characteristics of different land cover types and snow (Painter *et al.*, 2009). Unlike binary classifications that label pixels as fully snow-covered or snow-free, fSCA captures partial snow cover, offering higher spatial precision. This precision is especially beneficial for heterogeneous terrains with mixed snow and vegetation, where fSCA improves snow distribution estimates. By providing more detailed spatial information, fSCA enables more accurate hydrological modeling and enhances understanding of snowpack dynamics across diverse landscapes. Additionally, binary-format snow cover data can introduce significant uncertainties in climate, hydrological, and numerical weather models. The absence of fractional snow cover representation reduces these models' ability to accurately capture seasonal snow dynamics, particularly during snow accumulation and melt periods (Romanov *et al.*, 2003; Dietz *et al.*, 2012). To better integrate snow cover information into distributed physical models, fSCA maps need to be generated (Painter *et al.*, 2003; Dietz *et al.*, 2012).

Founded in 1986, the European Organisation for the Exploitation of Meteorological Satellites (EUMETSAT, https://www.eumetsat.int/) is the European operational satellite agency responsible for monitoring weather, climate, and the environment from space. EUMETSAT has also established cooperation with Earth observation satellite operators from Europe, China, India, Japan, Russia, South Korea, and the United States. To fully utilize the potential of EUMETSAT satellite data across a wide range of meteorological and environmental applications, serving the needs of its 30 Member States, a network of eight Satellite Application Facilities (SAFs) was established. Each SAF specializes in delivering products within a specific application area (https://www.eumetsat.int/about-us/satellite-application-facilities-safs).

The Support to Operational Hydrology and Water Management (H SAF, https://hsaf.meteoam.it/) program is one of the eight SAFs and was founded in 2005. H SAF includes 12 EUMETSAT member or cooperating states: Austria, Belgium, Bulgaria, Finland, France, Germany, Hungary, Italy, Poland, Romania, Slovakia, and Turkey. Additionally, the European Centre for Medium-Range Weather Forecasts (ECMWF) is part of this collaborative initiative. This broad membership reflects the strong commitment and cooperation among these entities to advance operational hydrology and water management through the use of satellite data and products (de Rosnay and Fairbairn, 2021).

The primary goal of H SAF is to develop innovative satellite-derived products with suitable temporal and spatial resolution to meet the demands of operational hydrology applications, using data from both current and future satellite missions. The program aims to improve the accuracy and efficiency of hydrological predictions and decision-making processes, enabling better management of water resources, flood forecasting, and related activities. By focusing on the production of reliable and timely satellite-derived products, H SAF plays a key role in enhancing the capabilities of operational hydrology and water management efforts. The satellite-derived products identified within H SAF include:

- Precipitation: This encompasses data on various forms of precipitation, such as liquid and solid (snow), as well as precipitation rates and accumulated amounts.
- Soil Moisture: H SAF provides information on soil moisture at the surface and in the root zone, which is critical for understanding water availability and soil-water dynamics.
- Snow-Related Parameters: The program offers essential data on snow cover, melting conditions, and snow-water equivalent, all of which are vital for snowpack monitoring and related hydrological applications.

The new generation daily operational fSCA product, H35, provided by the H SAF program, covers the entire Northern Hemisphere with a nominal horizontal resolution of 0.01° (i.e., ~1.1 km), and it is based on the multi-channel analysis of the Advanced Very High-Resolution Radiometer (AVHRR) instrument onboard NOAA and MetOp satellites (H-SAF_H35_PUM, 2020).

Validating a satellite-derived snow product is crucial for ensuring the accuracy and reliability of the data used in managing water resources, predicting weather and climate patterns, and assessing environmental changes (Kuter *et al.*, 2022, 2024). Without validation, the accuracy of the snow product remains uncertain, which can lead to incorrect interpretations and decisions. Validation involves comparing the satellite-derived data with ground-based measurements or high-resolution reference data (Brubaker *et al.*, 2005; Piazzi *et al.*, 2019). This process helps identify discrepancies, quantify the product's accuracy, and improve the algorithms used to generate the product.

This article aims to present the validation results for the H35 fSCA product over the Tibetan Platou (TP). The validation period spans the years 2019-2021. The reference dataset used in the validation is the daily snow cover products with no data gaps generated at a 500 m spatial resolution for TP from 2002 to 2021, which are based on long-term Moderate Resolution Imaging Spectroradiometer (MODIS) snow cover data (Huang *et al.*, 2018). The structure of the manuscript is as follows: Section 2 details the H35 product, the reference dataset used, and the validation methodology. Section 3 summarizes the results and discussions. Section 4 offers conclusions and suggests possible future research directions.

2. Materials and Methods

This section outlines the materials and methods used to validate the H35 product over TP. We provide a description of the H35 fSCA product and the reference dataset used for its validation. The methodology, data collection and processing procedures, and the statistical metrics applied are explained to offer a clear overview of the entire validation process.

2.1 The Tibetan Plateau

The Tibetan Plateau, often called the "Roof of the World" and the "Third Pole," is the highest and largest plateau on Earth. It covers an area of around 2.5 million square kilometers and has an average elevation of more than 4,500 meters above sea level (cf. Figure 1). It plays a critical role in global climate patterns and is home to some of the world's most important river systems, such as the Yangtze, Mekong, and Brahmaputra rivers, which provide water to millions of people in Asia (Liu *et al.*, 2022). The term "Third Pole" highlights the plateau's importance as the largest reservoir of freshwater outside the Arctic and Antarctic (Pan *et al.*, 2021). The region contains vast glaciers that serve as a crucial water source for surrounding regions (Yao *et al.*, 2012). However, climate change is accelerating glacier melt, which poses a serious threat to water availability downstream (Immerzeel *et al.*, 2010).

Formed by the collision of the Indian and Eurasian tectonic plates around 50 million years ago, the plateau continues to rise slowly due to ongoing tectonic activity. This region is also an active seismic zone, with frequent earthquakes and ongoing geological changes (Yin and Harrison, 2000)

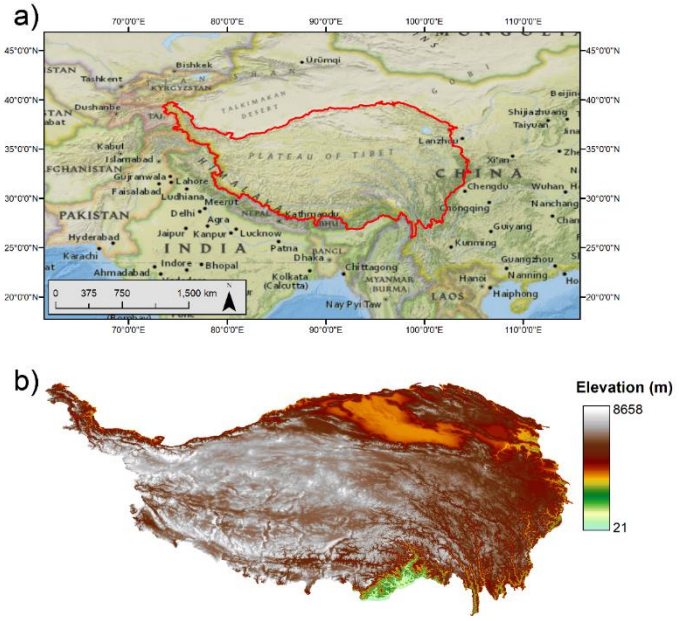

Figure 1. a) The Tibetan Plateou, and b) its DEM, which is MODIS MODDEMHKM product at 500 m resolution (Wolfe, 2013)

The Tibetan Plateau has a cold and dry climate, with long winters and short summers (Zhang *et al.*, 2020). Snow and glaciers cover large areas of the plateau, particularly in the western and northern parts. These glaciers are a key source of water for the rivers that flow into South and East Asia. As the glaciers shrink due to rising global temperatures, it could significantly affect the water supply in these regions (Yao *et al.*, 2012). The plateau is also an important region for biodiversity. Despite its harsh environment, it supports unique ecosystems, including species adapted to high altitudes like the snow leopard and the Tibetan antelope. However, human activities, such as grazing, agriculture, and infrastructure development, are putting pressure on these ecosystems (Xu *et al.*, 2009).

In recent years, the Tibetan Plateau has gained attention for its influence on atmospheric circulation, particularly the Asian monsoon system. Studies suggest that changes in the plateau's surface temperature and its snow cover can influence the timing and strength of monsoon rainfall, impacting agricultural production and water availability in many countries (Immerzeel *et al.*, 2010; Wu *et al.*, 2012).

2.2 The H35 fractional snow-covered area product

The daily operational H35 fSCA product offers 0.01° horizontal resolution, covering the Northern Hemisphere (cf. Figure 2). In contrast, its predecessor, H12, was limited to Pan-European coverage (H-SAF_H12_PUM, 2018). H35 is derived from the multi-channel analysis of the AVHRR instrument onboard NOAA and MetOp satellites. The AVHRR radiometer has an instantaneous field of view (IFOV) of 1.1 km at nadir, which increases to around 2 km near the edge of the 2900 km cross-track swath. The product is sampled at 0.01° intervals, resulting in an approximate resolution of 2 km, while the sampling distance is about 1 km (H-SAF_H35_PUM, 2020).

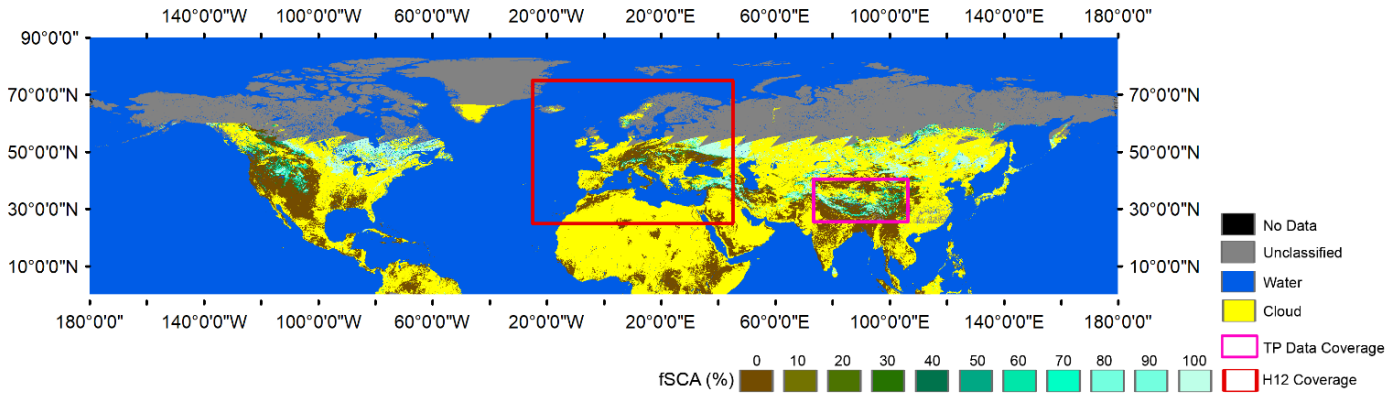

Figure 2. The H35 fSCA product on 13 February 2022, together with the spatial coverage of H12, and TP reference dataset employed in the validation

The H35 fSCA product relies on optical spectral channels to obtain fractional snow cover, which makes it vulnerable to cloud contamination, as clouds block surface visibility. Unlike microwave-based products, H35 cannot retrieve snow data through clouds, leading to data gaps. Additionally, being an operational snow product H35 lacks a gap-filling algorithm, limiting its effectiveness in regions with frequent cloud contamination.

The fSCA retrieval algorithm for H35 differs for flat/forested areas compared to mountainous regions. The Finnish Meteorological Institute (FMI) produces the H35 product for flat/forested areas, while the Turkish State Meteorological Service (TSMS) generates it for mountainous regions. Although both products cover the full H SAF area, they are combined at FMI. This merging integrates FMI's data for flat and forested regions with TSMS's data for mountainous areas, based on the provided mountain mask (H-SAF_H35_ATBD, 2020).

The fSCA product for flat/forested areas is based on an algorithm developed by FMI. This algorithm, detailed by Metsämäki *et al.* (2005), uses visible and near-infrared data and relies on a semi-empirical reflectance model. The model mathematically relates the reflectance from a given area to its fSCA value by incorporating reflectances from different sources, including wet snow, forest canopy, and snow-free ground.

In mountainous regions, factors such as the sun's zenith and azimuth angles, as well as the observation direction relative to these angles, significantly impact the observed signals. These factors pose greater challenges to snow retrieval accuracy in mountainous areas compared to forested regions. The algorithm for mountainous regions was developed by the Middle East Technical University (METU) and implemented within the TSMS infrastructure. This fSCA algorithm employs a sub-pixel reflectance model, where pixel reflectance is expressed as a linear combination of snow and snow-free bare ground. The model, initially proposed by Vikhamar *et al.* (2004), was based on a linear mixture of snow, individual tree species, and snow-free bare ground. For the fSCA algorithm, the focus is primarily on the interaction between snow and snow-free bare ground reflectance, using this simplified approach to estimate snow cover proportion accurately within each pixel.

2.3 Reference dataset employed in the validation

The validation process of the H35 product over TP is realized by comparing it with the daily cloud-free snow cover product developed by Yan and Jianghui (2022). This daily binary snow product with no data gaps at a 500 m spatial resolution for TP from 2002 to 2021 is based on long-term MODIS snow cover data. The product spans the area delineated by latitudes 26°00′12″ N - 39°46′50″ N, and longitudes 73°18′52″ E - 104°46′59″ E (cf. Figure 3). The product was accomplished through a Hidden Markov Random Field (HMRF) modeling technique, which effectively integrates spectral, spatiotemporal, and environmental information as explained in detail in Huang *et al.* (2018). The HMRF framework not only fills data gaps caused by frequent cloud cover, but also enhances the accuracy of the original MODIS snow cover data.

A key feature of this approach is the incorporation of solar radiation as an environmental context, which improves snow identification accuracy in mountainous areas. Validation against in-situ observations and Landsat-8 OLI-derived snow cover showed that the new product achieved accuracies of 98.31% and 92.44%, respectively. This new snow cover product is particularly more accurate during the snow transition period and in complex terrains, including higher elevations and sunny slopes. This gap-free product improves the spatiotemporal continuity and accuracy in challenging terrains of the original MODIS snow data, providing a reliable foundation for studying climate change and hydrological cycles in TP (Yan and Jianghui, 2022).

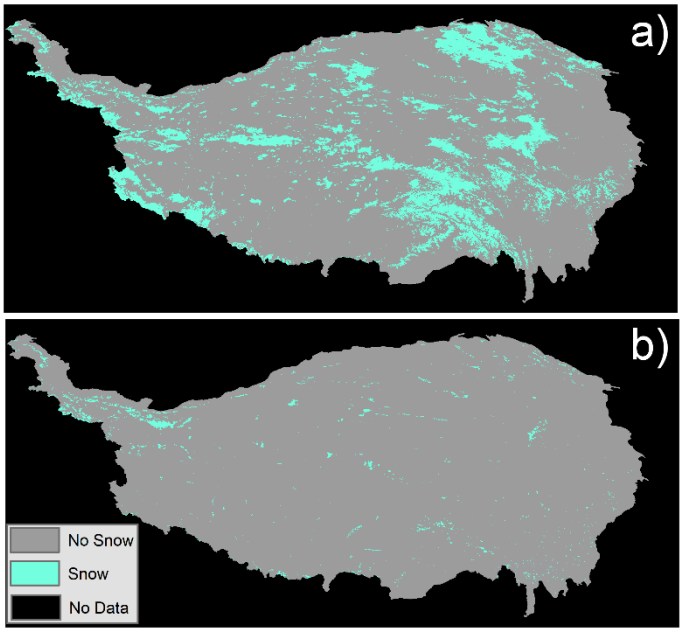

Figure 3. The HMRF-based reference binary snow cover data over TP on a) 1 January 2020, and b) 17 August 2020

2.4 The validation methodology

Since the H35 is an fSCA product, where the pixel values range from 0% to 100%, and the reference product over TP is in the form of daily binary snow cover maps, the following methodology is employed during the validation:

- The reference daily binary snow cover maps are resampled to the original resolution of the H35 product using the nearest neighborhood method.
- Then, for a given date, each valid pixel of H35 product is converted to a binary snow value by labeling fSCA ranges < 50% as no snow, otherwise snow.
- H35 pixels labeled as cloud, water, no data and unclassified are excluded from the analysis.

There are several thresholds proposed in the literature for the conversion from fSCA to binary snow, which are 0%, 10%, 15%, 0.30 and 50% (Rittger *et al.*, 2013; Xiao *et al.*, 2022; Stillinger *et al.*, 2023). In this study, 50% threshold is applied.

The performance of the H35 product is then compared with the reference binary snow maps by using the following dichotomous metrics (Doswell III *et al.*, 1990; Fawcett, 2006) derived from the associated binary error matrices (cf. Table 1):

- Probability of detection (POD) = A/(A+C),
- False alarm ratio (FAR) = B/(A+B),
- Accuracy (ACC) = (A+D)/(A+B+C+D).

The validation period covers three consecutive years, 2019, 2020 and 2021. As the H35 production started in May 2019, the validation for 2019 covers the period between May and December. However, during the three-year validation period, higher False Alarm Ratio (FAR) values are observed between July and September. These months correspond to the melting season over the TP, resulting in minimal snow-covered area percentages (cf. Figure 3b). Furthermore, certain dates exhibit a high percentage of "no data" pixels, limiting the number of observations available for validation. This limitation naturally contributes to elevated FAR and lower POD values. To address these issues, the validation metrics are calculated by excluding data from June to September. Additionally, dates with a percentage of available pixels below a specified threshold are excluded from the analysis to ensure more reliable results.

Table 1. A sample binary error matrix

		Reference Data over TP	
		Snow	**No snow**
H35 product	**Snow**	HITS (A)	FALSE ALARMS (B)
	No snow	MISSES (C)	CORRECT NEGATIVES (D)

3. Results and Discussions

The overall validation results in terms of POD, FAR and ACC metrics for the H35 product over TP during the whole analysis period (i.e., from May 2019 to December 2021) are illustrated in Figure 4. During the 2019-2020 snow season, the lowest POD metrics are observed between May and June 2019. In October, POD values start to increase and reach their peak during December (~ 0.91), and then follow an almost stable trend till the end of March 2020. As of early April 2020, POD values enter a downward trend again and reach their minimum value in June 2020 (~ 0.15).

The 2020-2021 snow season over the TP exhibits a slightly different behavior than the previous one. As mid-October 2020, PODs start to rise but reach its peak in early April 2021 (~ 0.91), almost three months later as compared to the previous snow season. Starting from late April 2021, the PODs go into a descending trend again and the minimum value is observed in mid-October 2021 (~ 0.36), which is relatively higher than that of the previous snow season.

As expected, the FARs over the TP show reverse mirror image trend. For the 2019-2020 snow season, FARs begin to increase in mid-May and reach the peak value of ~ 0.53 in early-October. The minimum FAR is ~ 0.14, reached on 1st of February 2020, and from this day, it starts to increase gradually up to ~ 0.54, in late-October 2020. The lowest FAR during the whole analysis period is ~ 0.11, in mid-December 2021

Unlike the monthly fluctuations seen in the POD and FAR values, the ACC values remain relatively stable from May 2019 to December 2021, staying mostly within the range of 0.8 – 1.0. The highest recorded ACCs for the 2019-2020 and 2020-2021 snow seasons are 0.98 and 0.99, respectively. The 2020-2021 snow season shows more fluctuations compared to the previous season, with greater variability. The lowest accuracy value for the entire analysis period is recorded in early-April 2021 (i.e., 0.74).

Figure 5 shows the spatial distribution of the POD, FAR, and ACC metrics, along with the percentage of cloudy days for each year over the TP. The yearly POD, FAR, and ACC values are generated by summing the total counts of A, B, C, and D values (cf. Table 1) for each valid pixel. Invalid H35 pixels (e.g., cloud, water, no data) are excluded from these calculations.

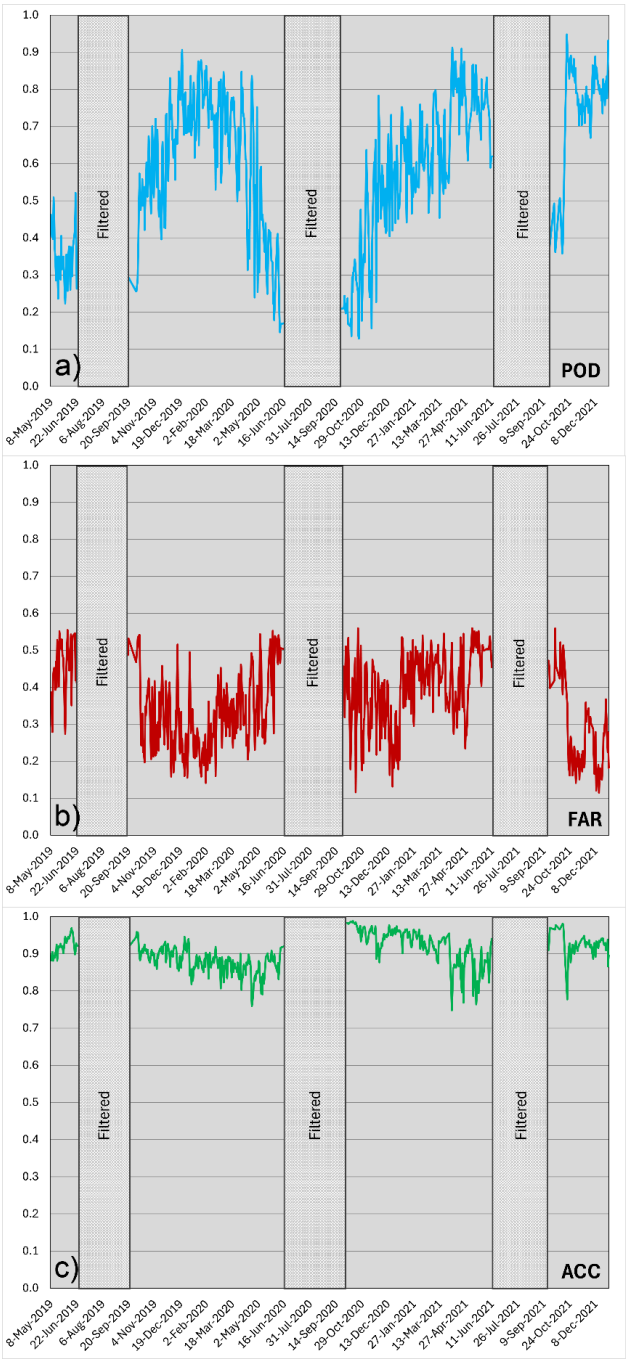

Figure 4. The overall accuracy metrics between May 2019 and December 2021: a) POD, b) FAR, and c) ACC

Meanwhile, the cloud-cover percentage for each pixel is determined by summing the number of cloudy days for that pixel and dividing it by the total number of days in the corresponding year. When reviewing the illustrations for 2019 in Figure 5, it is important to note that the H35 dataset only covers the period from May to December of that year.

The POD values in 2019 are relatively lower compared to those in 2020 and 2021. In the mid-northern, southern, and southeastern regions, lower PODs are observed. However, the POD values in 2021 are clearly better than those in 2020. The distribution of FAR values in 2019 and 2020 shows a similar pattern, with low FARs spread across the entire TP, primarily over the mid and northern latitudes. However, in 2021, the FARs become more concentrated in the northwestern areas. The accuracy values for each year follow a similar distribution pattern across the entire TP, with a yearly decline observed in the high-altitude mid-southern region.

The spatial distribution of cloud-cover percentage in 2019 and 2020 is nearly identical. However, 2021 shows a significant increase in cloud cover across the entire TP, particularly in the southeastern region.

The higher False Alarm Rate (FAR) values observed during the summer months may be influenced by two main factors: cloud misclassification and changes in surface reflectance due to the melting of snow. During the summer, particularly from May to September, cloud cover tends to be more frequent, especially in the southeastern regions of the TP, as shown in Figure 5. Although the H35 product is designed to detect snow cover, it relies on optical spectral channels that are highly susceptible to cloud contamination. As a result, clouds may be incorrectly classified as snow, leading to an increase in FAR.

In addition to cloud misclassification, the summer months coincide with the snowmelt period, where the transition from snow-covered surfaces to exposed vegetation occurs. This change in surface reflectance can cause snow pixels to appear less distinct or even misclassified as non-snow. As snow melts, the underlying vegetation or soil may have a similar spectral signature to partially snow-covered areas, contributing to the increase in FAR during this period.

The spatial distribution of FAR in 2021, with higher concentrations in the northwestern regions, may also reflect these surface changes, where mixed snow and vegetation patterns are more prevalent. Given that the H35 product does not include a gap-filling algorithm, missing data due to cloud cover can further contribute to the higher FAR, especially in regions with significant cloud cover during the summer months.

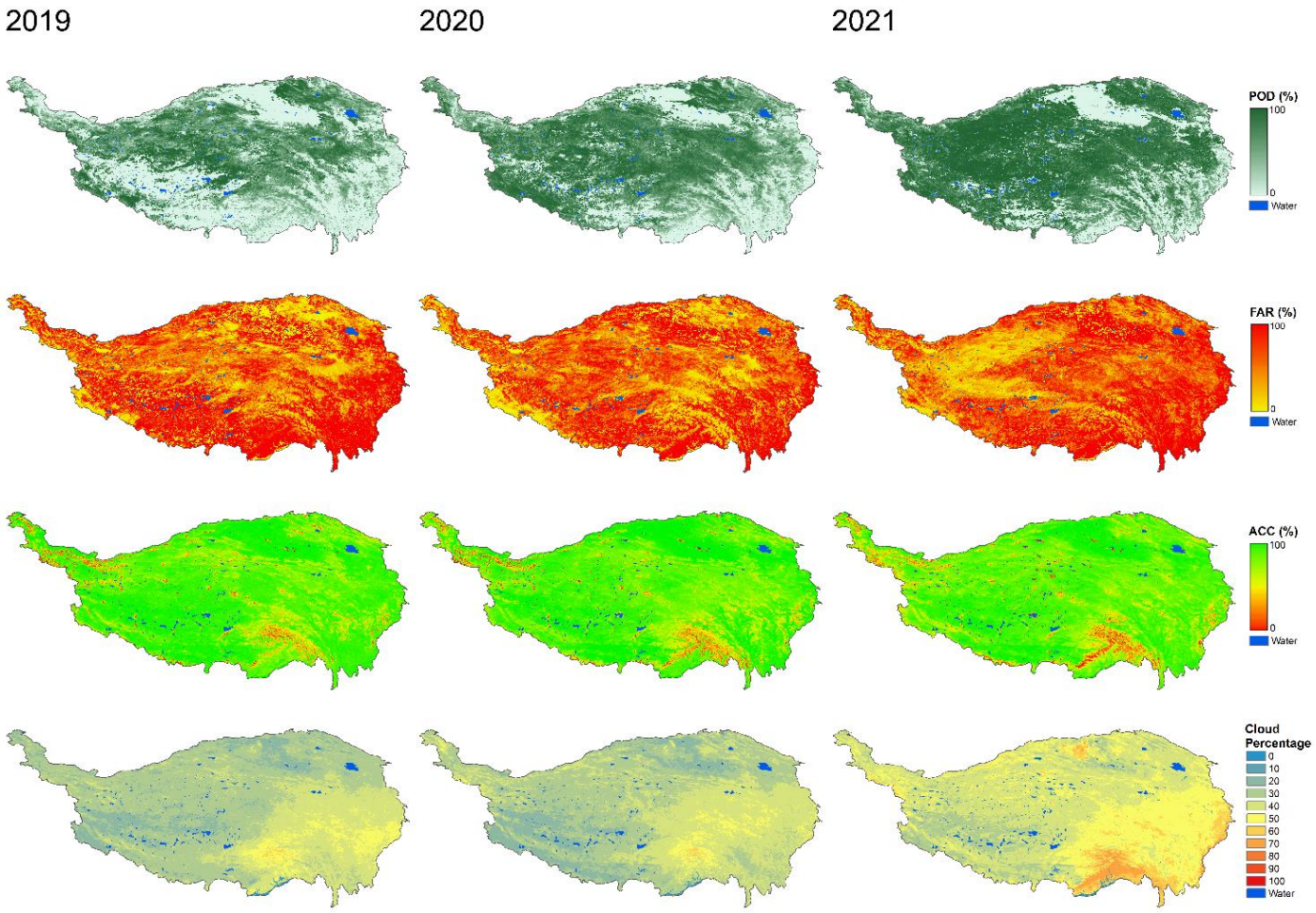

Figure 5. From top to bottom: The spatial distribution of POD, FAR, ACC metrics, and cloud-covered day percentages

Integrating machine learning (ML) models for cloud detection has shown promising results in improving the performance of snow products derived from remote sensing data. Since snow and cloud cover often exhibit similar characteristics in optical channels, traditional snow detection algorithms can struggle with cloud contamination. Machine learning techniques, such as convolutional neural networks (CNNs), have been proposed for more accurate differentiation between snow and clouds in remote sensing images (Zhu and Woodcock, 2014; Matsunobu *et al.*, 2021; Yu and Lary, 2021). These methods leverage multi-scale feature fusion to enhance the model's ability to distinguish between these two types of cover. By integrating such models into existing snow detection systems, the accuracy of snow products could be significantly improved, especially in areas where cloud contamination is a persistent issue. Cloud detection models could filter out false positives in snow mapping, resulting in more reliable snow cover estimates. Additionally, these models can be trained to handle the seasonal and geographical variability of cloud and snow cover, providing more robust snow detection during periods of cloud cover.

4. Conclusions

The validation of satellite-derived snow products is crucial for ensuring the reliability and accuracy of remote sensing data in snow hydrology studies. In this study, we assessed the performance of the EUMATSAT H SAF H35 fSCA product over the TP from May 2019 to December 2021. By comparing the H35 fSCA estimates with a reference snow cover dataset based on MODIS data and validated through in-situ observations, we aimed to establish the accuracy and fidelity of the H35 product. This validation provides valuable insights into the product's capability for monitoring snow cover in this complex and high-altitude region.

The results show that the H35 product performs well in detecting snow cover across the region, but there are some seasonal and spatial variations in accuracy. The probability of detection (POD) and accuracy (ACC) are generally high during the snow seasons, with peak values observed in the winter months. However, lower POD values occur during the summer, particularly in areas with minimal snow cover. The false alarm ratio (FAR) shows a reverse trend, being higher during the summer months.

Spatial analysis of the metrics reveals some variability across the Tibetan Plateau. Lower POD values are found in the mid-northern and southeastern areas, while accuracy decreases in high-altitude regions. Cloud cover significantly impacts the results, especially in 2021, where an increase in cloud-covered days was observed.

Despite these challenges, the EUMETSAT's H35 product demonstrates reliable performance for snow detection over the TP. Future improvements could focus on enhancing accuracy in complex terrain and addressing the limitations posed by cloud

cover. The validated H35 product can serve as a valuable tool for studying snow cover dynamics in the region, which is important for understanding hydrological and climate processes.

These validation efforts are essential for enhancing the credibility of satellite-derived snow products and expanding their applicability in hydrological and environmental studies. Additionally, the contributions of EUMETSAT H SAF in developing accurate and reliable snow products highlight the significance of collaborative efforts in advancing scientific knowledge. H SAF's commitment to producing high-quality snow data has established a foundation for multidisciplinary research and operational applications in snow hydrology.

References

Breen, C., Vuyovich, C., Odden, J., Hall, D., Prugh, L., 2023. Evaluating MODIS snow products using an extensive wildlife camera network. Remote Sensing of Environment, 295, 113648.

Brown, R.D., Mote, P.W., 2009. The response of northern hemisphere snow cover to a changing climate. Journal of Climate, 22, 2124-2145.

Brubaker, K.L., Pinker, R.T., Deviatova, E., 2005. Evaluation and comparison of MODIS and IMS snow-cover estimates for the continental United States Using Station Data. Journal of Hydrometeorology, 6, 1002-1017.

Chen, X., Yang, Y., Yin, C., 2021. Contribution of changes in snow cover extent to shortwave radiation perturbations at the top of the atmosphere over the northern hemisphere during 2000–2019. Remote Sensing Letters, 13, 4938.

de Rosnay, P., Fairbairn, D., 2021. H SAF web page. Available at: https://confluence.ecmwf.int/display/LDAS/H+SAF, Accessed on 1 August, 2023.

Dietz, A.J., Kuenzer, C., Gessner, U., Dech, S., 2012. Remote sensing of snow – a review of available methods. International Journal of Remote Sensing, 33, 4094-4134.

Doswell III, C.A., Davies-Jones, R., Keller, D.L., 1990. On summary measures of skill in rare event forecasting based on contingency tables. Weather and Forecasting, 5, 576-585.

Fawcett, T., 2006. An introduction to ROC analysis. Pattern recognition letters, 27, 861-874.

H-SAF_H12_PUM, 2018. Product User Manual (PUM) for product H12 – SN-OBS-3 Effective snow cover by VIS/IR radiometry. Available at: https://hsaf.meteoam.it/Products/Detail?prod=H12, Accessed on 30 August, 2023.

H-SAF_H35_ATBD, 2020. Algorithm Theoretical Baseline Document (ATBD) for product H35 – FSC-H Effective snow cover by VIS/IR radiometry. Available at: https://hsaf.meteoam.it/Products/Detail?prod=H35, Accessed on 30 August, 2023.

H-SAF_H35_PUM, 2020. Product User Manual (PUM) for product H35 – SN-OBS-1P Effective snow cover by VIS/IR radiometry. Available at: https://hsaf.meteoam.it/Products/Detail?prod=H35, Accessed on 30 August, 2023.

Hall, D.K., Riggs, G.A., Salomonson, V.V., 1995. Development of Methods for Mapping Global Snow Cover Using Moderate Resolution Imaging Spectroradiometer Data. Remote Sensing of Environment, 54, 127-140.

Huang, Y., Liu, H., Yu, B., Wu, J., Kang, E.L., Xu, M., Wang, S., Klein, A., Chen, Y., 2018. Improving MODIS snow products with a HMRF-based spatio-temporal modeling technique in the Upper Rio Grande Basin. Remote Sensing of Environment, 204, 568-582.

Immerzeel, W.W., van Beek, L.P.H., Bierkens, M.F.P., 2010. Climate change will affect the asian water towers. Science, 328, 1382-1385.

Kuter, S., Akyurek, Z., Weber, G.W., 2018. Retrieval of fractional snow covered area from MODIS data by multivariate adaptive regression splines. Remote Sensing of Environment, 205, 236-252.

Kuter, S., Karaman, Ç.H., Akpınar, M.B., Akyürek, Z., 2022. Validation of EUMETSAT H-SAF space-born snow water equivalent product (H13) for the 2020-2021 snow year over Turkey. Anadolu Orman Araştırmaları Dergisi, 8, 16-21.

Kuter, S., Karaman, Ç.H., Akpınar, M.B., Akyürek, Z., 2024. From Anatolian Plateau to American Plains: A transcontinental assessment of the EUMETSAT H SAF's new generation snow water equivalent product over Türkiye and the conterminous U.S. Anadolu Orman Araştırmaları Dergisi, 9, 33-40.

Liu, J., Milne, R.I., Zhu, G.-F., Spicer, R.A., Wambulwa, M.C., Wu, Z.-Y., Boufford, D.E., Luo, Y.-H., Provan, J., Yi, T.-S., Cai, J., Wang, H., Gao, L.-M., Li, D.-Z., 2022. Name and scale matter: Clarifying the geography of Tibetan Plateau and adjacent mountain regions. Global and Planetary Change, 215, 103893.

Matsunobu, L.M., Pedro, H.T.C., Coimbra, C.F.M., 2021. Cloud detection using convolutional neural networks on remote sensing images. Solar Energy, 230, 1020-1032.

Metsämäki, S., Pulliainen, J., Salminen, M., Luojus, K., Wiesmann, A., Solberg, R., Böttcher, K., Hiltunen, M., Ripper, E., 2015. Introduction to GlobSnow Snow Extent products with considerations for accuracy assessment. Remote Sensing of Environment, 156, 96-108.

Metsämäki, S.J., Anttila, S.T., Markus, H.J., Vepsäläinen, J.M., 2005. A feasible method for fractional snow cover mapping in boreal zone based on a reflectance model. Remote Sensing of Environment, 95, 77-95.

Painter, T.H., Dozier, J., Roberts, D.A., Davis, R.E., Green, R.O., 2003. Retrieval of subpixel snow-covered area and grain size from imaging spectrometer data. Remote Sensing of Environment, 85, 64-77.

Painter, T.H., Rittger, K., McKenzie, C., Slaughter, P., Davis, R.E., Dozier, J., 2009. Retrieval of subpixel snow covered area, grain size, and albedo from MODIS. Remote Sensing of Environment, 113, 868-879.

Pan, X., Guo, X., Li, X., Niu, X., Yang, X., Feng, M., Che, T., Jin, R., Ran, Y., Guo, J., Hu, X., Wu, A., 2021. National Tibetan Plateau Data Center: promoting earth system science on the third pole. Bulletin of the American Meteorological Society, 102, E2062-E2078.

Piazzi, G., Tanis, C.M., Kuter, S., Simsek, B., Puca, S., Toniazzo, A., Takala, M., Akyürek, Z., Gabellani, S., Arslan, A.N., 2019. Cross-Country Assessment of H-SAF Snow Products by Sentinel-2 Imagery Validated against In-Situ Observations and Webcam Photography. Geosciences, 9, 129.

Pulliainen, J., Hallikainen, M., 2001. Retrieval of Regional Snow Water Equivalent from Space-Borne Passive Microwave Observations. Remote Sensing of Environment, 75, 76-85.

Pulliainen, J., Luojus, K., Derksen, C., Mudryk, L., Lemmetyinen, J., Salminen, M., Ikonen, J., Takala, M., Cohen, J., Smolander, T., Norberg, J., 2020. Patterns and trends of Northern Hemisphere snow mass from 1980 to 2018. Nature, 581, 294-298.

Rittger, K., Painter, T.H., Dozier, J., 2013. Assessment of methods for mapping snow cover from MODIS. Advances in Water Resources, 51, 367-380.

Romanov, P., Tarpley, D., Gutman, G., Carroll, T., 2003. Mapping and monitoring of the snow cover fraction over North America. Journal of Geophysical Research: Atmospheres, 108.

Saberi, N., Kelly, R., Flemming, M., Li, Q., 2020. Review of snow water equivalent retrieval methods using spaceborne passive microwave radiometry. International Journal of Remote Sensing, 41, 996-1018.

Stillinger, T., Rittger, K., Raleigh, M.S., Michell, A., Davis, R.E., Bair, E.H., 2023. Landsat, MODIS, and VIIRS snow cover mapping algorithm performance as validated by airborne lidar datasets. The Cryosphere, 17, 567-590.

Takala, M., Luojus, K., Pulliainen, J., Derksen, C., Lemmetyinen, J., Kärnä, J.-P., Koskinen, J., Bojkov, B., 2011. Estimating northern hemisphere snow water equivalent for climate research through assimilation of space-borne radiometer data and ground-based measurements. Remote Sensing of Environment, 115, 3517-3529.

Tekeli, A.E., Akyürek, Z., Şorman, A.A., Şensoy, A., Şorman, Ü., 2005. Using MODIS snow cover maps in modeling snowmelt runoff process in the eastern part of Turkey. Remote Sensing of Environment, 97, 216-230.

Vikhamar, D., Solberg, R., Seidel, K., 2004. Reflectance modeling of snow-covered forests in hilly terrain. Photogrammetric Engineering & Remote Sensing, 70, 1069-1079.

Wang, Y., Huang, X., Liang, H., Sun, Y., Feng, Q., Liang, T., 2018. Tracking snow variations in the northern hemisphere using multi-source remote sensing data (2000–2015). Remote Sens-Basel, 10, 136.

Wolfe, R., 2013. MODIS Land Digital Elevation Model and Land/Water Mask in the Sinusoidal Grid Version 6.0. Available at: https://landweb.modaps.eosdis.nasa.gov/data/userguide/DEM.pdf, Accessed on 30 August 2024,

Wu, G., Liu, Y., He, B., Bao, Q., Duan, A., Jin, F.-F., 2012. Thermal controls on the asian summer monsoon. Scientific Reports, 2, 404.

Xiao, X., He, T., Liang, S., Liu, X., Ma, Y., Liang, S., Chen, X., 2022. Estimating fractional snow cover in vegetated environments using MODIS surface reflectance data. International Journal of Applied Earth Observation and Geoinformation, 114, 103030.

Xu, J., Grumbine, R.E., Shrestha, A., Eriksson, M., Yang, X., Wang, Y.U.N., Wilkes, A., 2009. The melting Himalayas: cascading effects of climate change on water, biodiversity, and livelihoods. Conservation Biology, 23, 520-530.

Yan, H., Jianghui, X., 2022. Daily cloud-free snow cover products for Tibetan Plateau from 2002 to 2021. A Big Earth Data Platform for Three Poles Available at: https://dx.doi.org/10.11888/Cryos.tpdc.272204, Accessed on 1 January 2024,

Yao, T., Thompson, L., Yang, W., Yu, W., Gao, Y., Guo, X., Yang, X., Duan, K., Zhao, H., Xu, B., Pu, J., Lu, A., Xiang, Y., Kattel, D.B., Joswiak, D., 2012. Different glacier status with atmospheric circulations in Tibetan Plateau and surroundings. Nature Climate Change, 2, 663-667.

Yin, A., Harrison, T.M., 2000. Geologic evolution of the Himalayan-Tibetan Orogen. Annual Review of Earth and Planetary Sciences, 28, 211-280.

Yu, X., Lary, D.J., 2021. Cloud detection using an ensemble of pixel-based machine learning models incorporating unsupervised classification. Remote Sens-Basel, 13.

Zhang, G., Yao, T., Xie, H., Yang, K., Zhu, L., Shum, C.K., Bolch, T., Yi, S., Allen, S., Jiang, L., Chen, W., Ke, C., 2020. Response of Tibetan Plateau lakes to climate change: Trends, patterns, and mechanisms. Earth-Science Reviews, 208, 103269.

Zhu, Z., Woodcock, C.E., 2014. Automated cloud, cloud shadow, and snow detection in multitemporal Landsat data: An algorithm designed specifically for monitoring land cover change. Remote Sensing of Environment, 152, 217-234.